

BLENDING IN FUTURE SPACE-BASED MICROLENSING SURVEYS

CHEONGHO HAN¹, BYEONG-GON PARK², HO-IL KIM², AND KYONGAE CHANG³

Draft version November 28, 2018

ABSTRACT

We investigate the effect of blending in future gravitational microlensing surveys by carrying out simulation of Galactic bulge microlensing events to be detected from a proposed space-based lensing survey. From this simulation, we find that the contribution of the flux from background stars to the total blended flux will be equivalent to that from the lens itself despite the greatly improved resolution from space observations, implying that characterizing lenses from the analysis of the blended flux would not be easy. As a method to isolate events for which most of the blended flux is attributable to the lens, we propose to use astrometric information of source star image centroid motion. For the sample of events obtained by imposing a criterion that the centroid shift should be less than three times of the astrometric uncertainty among the events for which blending is noticed with blended light fractions $f_B > 0.2$, we estimate that the contamination of the blended flux by background stars will be less than 20% for most ($\sim 90\%$) of the sample events. The expected rate of these events is $\gtrsim 700$ events/yr, which is large enough for the statistical analysis of the lens populations.

Subject headings: gravitational lensing

1. INTRODUCTION

Observational experiments to detect light variations of stars induced by gravitational microlensing have been and are being carried out for more than a decade (Udalski et al. 1993; Alcock et al. 1993; Aubourg et al. 1993; Bond et al. 2001). Originally, the experiments were initiated for the purpose of searching for dark matter in the Galactic halo (Paczynski 1986). However, microlensing developed many applications in various aspects of galactic, stellar, and planetary astrophysics such as probing the structure of the inner galaxy (Kiraga & Paczynski 1994; Evans 1994; Han & Gould 1995b; Zhao, Spergel, & Rich 1995), resolving the photosphere of distant stars (Witt 1995; Albrow et al. 1999; Abe et al. 2003; Field et al. 2003), and detecting extrasolar planets (Mao & Paczynski 1991; Gould & Loeb 1992; Bond et al. 2004; Udalski et al. 2005; Beaulieu et al. 2006; Gould et al. 2006). Current experiments are routinely detecting more than 500 events every season and the total number of detected events is now reaching 3000.

The probability of a star being gravitationally lensed is very low (of the order of 10^{-6}). As events are very rare, lensing searches are conducted toward very crowded star fields such as the Galactic bulge in order to monitor as many stars as possible within a single frame. For observations in such a dense field, blending of stellar images is inevitable (Di Stefano & Esin 1995; Woźniak 1997). The lightcurve of a blending-affected event is expressed as

$$F_{\text{obs}} = AF_0 + F_B; \quad A = \frac{u^2 + 2}{u(u^2 + 4)}, \quad (1)$$

where F_0 is the baseline flux of the lensed source star, F_B is the amount of the blended flux, A is the magnification induced by lensing, and u is the lens-source separation normalized by

the Einstein ring radius θ_E . The normalized lens-source separation is related to the lensing parameters by

$$u = \left[\left(\frac{t - t_0}{t_E} \right)^2 - u_0^2 \right]^{1/2}, \quad (2)$$

where t_E is the Einstein timescale, t_0 is the time of the closest lens-source approach, and u_0 is the separation at that moment (impact parameter). Among the lensing parameters, the Einstein timescale is related to the mass and location of the lens and relative lens-source transverse speed, and thus it can provide constraint about the lens system. However, the constraint is weak because the timescale results from the combination of the physical parameters. Blending aggravates the photometric precision due to the increased noise from the blended flux. In addition, blending causes accurate determinations of the lensing parameters difficult due to the poorly known baseline flux of the source star. As a result, the constraint about the lens system becomes further weaker.

Recently, next-generation microlensing experiments based in space are being seriously discussed. *Microlensing Planet Finder (MPF)*, that succeeds the original concept of *Galactic Exoplanet Survey Telescope (GEST)* mission (Bennett & Rhie 2002), is a space mission proposed to NASA's Discovery Program with the main goal of searching for a large sample of extrasolar planets by using gravitation lensing method (Bennett 2004). By conducting observations in space, it is possible to minimize blending effect thanks to the improved resolution. Another important advantage of the space observation may be that one can directly detect and characterize the lens based on the observed flux. This is possible when a light-emitting star is responsible for a lensing event and the flux from the lens contributes a substantial fraction of the observed flux. It is believed that majority of events detected toward the Galactic bulge are caused by stars (Han & Gould 2003). In addition, the *MPF* mission plans to monitor faint main-sequence stars in order to optimize detections of low-mass planets by minimizing finite-source effect. Therefore, the light from the lens would not be negligible for a significant fraction of the event sample, and thus the existence of the lens could be revealed by the excess flux from the lens. By conducting multi-band

¹ Program of Brain Korea 21, Department of Physics, Institute for Basic Science Research, Chungbuk National University, Chongju, Korea 361-763; cheongho@astroph.chungbuk.ac.kr

² Korea Astronomy and Space Science Institute, Hwaam-Dong, Yuseong-Gu, Daejeon, Korea 305-348; bgpark,hikim@kasi.re.kr

³ Department of Physics, Chongju University, Chongju, Korea 360-764; kchang@chongju.ac.kr

observations, it would be possible to determine the spectral type of the lens, which would provide much tighter constraint about the lens.

However, this new method of constraining lenses can be applicable under the condition that source stars to be observed are in most cases free from blending by the flux of blends other than lenses. If an unrelated background star is located within the resolution disk of the lensed source star, the blended flux comes not only from the lens but also from the background star. This causes complexity in the analysis of the observed blended light, making it difficult to uniquely characterize the lens. Han (2005) (hereafter Paper I) warned of the possible contamination of the blended flux by background stars. As a method to resolve the contamination, he suggested to use the astrometric information of the source star image centroid shift. If an event is affected by background stellar blending, the centroid will shift from the apparent position of the combined image of the source plus blended stars toward the lensed star during the event (Goldberg 1998).

In this paper, we further investigate the blending problem in future space-based lensing surveys following Paper I and probe the feasibility of sorting out events whose blended flux is mostly attributable to the lenses by using the additional astrometric information of the centroid shift. For this, we carry out simulation of Galactic bulge microlensing events expected to be detected from the proposed *MPF* survey by imposing realistic observational conditions and detection criteria. Based on this simulation, we investigate the expected pattern of blending and the seriousness of the contamination by background stars. We also estimate the fraction of events that can be identified to be free from background stellar blending by using the proposed method.

2. SIMULATION

The basics scheme of the simulation of lensing events is similar to the one in Paper I. The locations of the lenses and source stars are allocated based on Han & Gould (1995a) Galactic mass distribution model, that is composed of a double-exponential disk and a barred bulge. The velocity distribution of the bulge is deduced from the tensor virial theorem, while the disk velocity distribution is modeled to have a flat rotation speed of $v_c = 220 \text{ km s}^{-1}$ and velocity dispersion along and normal to the disk plane of $\sigma_{\parallel} = 30 \text{ km s}^{-1}$ and $\sigma_{\perp} = 20 \text{ km s}^{-1}$, respectively. The brightnesses of the bulge stars are assigned on the basis of a combined luminosity function of constructed based on those of Holtzman et al. (1998) and Gould, Bahcall, & Flynn (1997) considering extinction and distance modulus. The lens masses are assigned based on the mass function of Gould (2000), which is composed of stars and stellar remnants. The mass function model is constructed under the assumption that bulge stars are formed initially according to a double power-law distribution of $dN/dM = k(M/0.7 M_{\odot})^{\gamma}$, where $\gamma = -2.0$ for $M \geq 0.7 M_{\odot}$ and $\gamma = -1.3$ for $M < 0.7 M_{\odot}$. Based on this initial mass function, remnants are modeled by assuming that the stars with initial masses $1 M_{\odot} < M < 8 M_{\odot}$, $8 M_{\odot} < M < 40 M_{\odot}$, and $M > 40 M_{\odot}$ have evolved into white dwarfs (with a mean mass $\langle M \rangle = 0.6 M_{\odot}$), neutron stars ($\langle M \rangle = 1.35 M_{\odot}$), and black holes ($\langle M \rangle = 5 M_{\odot}$), respectively. For events caused by stellar lenses, the lens brightness is determined based on the lens mass by using a mass-luminosity relation. For events caused by remnant lenses, the lens is assumed to be dark.

However, the main focus of Paper I was investigating possible contamination of blended flux in general and thus it is

not focused on a specific survey. As a result, there are several major differences between the simulations in Paper I and this work. The differences are described below.

1. Since no specific instrument was defined, the analysis in Paper I was based on all possible events regardless of their detectability. In this work, analysis are based only on events that could be detected from the *MPF* survey. The detectability of an events is subject to the condition and strategy of observation. For the observation field, we assume that the future survey will monitor toward a field centered at $(l, b) \sim (1.2^{\circ}, -2.4^{\circ})$ with a field of view of $(\Delta l, \Delta b) \sim (0.93^{\circ}, 2.8^{\circ})$. For a sampling frequency, we assume that the survey will continuously observe the target field with an interval of 15 minutes during 9 months of a year. For each interval, we assume that a 10-minute exposure image is acquired with a photon count rate of 13 photons/sec for an $I = 22$ star.
2. Another factor that determines the event detectability is the selection criteria. We judge the detectability of an event based on the uncertainties of the lensing parameters recovered from the lightcurve. We determine the uncertainties by computing the curvature matrix of χ^2 surface of the lensing parameters for each event produced by the simulation. For the case of a lensing lightcurve, the curvature matrix is defined as

$$b_{ij} = \sum_k^{N_{\text{obs}}} \frac{\partial F_{\text{obs},k}}{\partial p_i} \frac{\partial F_{\text{obs},k}}{\partial p_j} \frac{1}{\sigma_k^2}, \quad (3)$$

where N_{obs} is the number of observations, $\sigma_k = \sqrt{F_{\text{obs}}}$ is the photometric precision of each measurement, and $p_i \equiv (F_0, F_B, u_0, t_0, t_E)$ are the five lensing parameters required to fit the lightcurve of a standard point-source single-lens event. Then, the uncertainties of the individual lensing parameters correspond to the diagonal components of the inverse curvature matrix (covariance matrix), i.e.

$$\sigma_{p_i} = \sqrt{c_{ii}}; \quad c \equiv b^{-1}. \quad (4)$$

With the determined uncertainties, we set the detection criteria of events such that the fractional uncertainties of the timescale and blended flux should be less than 20%, i.e. $\sigma_{t_E}/t_E \leq 0.2$ and $\sigma_{F_B}/F_{\text{obs}} \leq 0.2$. Under this definition of event detectability, we note that events can be detected even when the source star trajectory does not enter the Einstein ring of the lens. This can be seen in the upper left panel of Figure 1, where we present the distribution of impact parameters of events. From the distribution, one finds that a fraction of events have impact parameters larger than unity, especially for events involved with relatively bright source stars ($I_0 \lesssim 22$). In Paper I, detectable events were limited only to those with source trajectories entering the Einstein ring, i.e. $u_0 < 1.0$.

3. Another major difference is the brightness range of source stars. In Paper I, we considered only stars with *I*-band baseline brightness of $I_0 \lesssim 23$. With the implementation of the detection criteria described above, we found that events associated with much fainter stars could be detected. In this work, we, therefore, do not set the limit of source star brightness as long as the

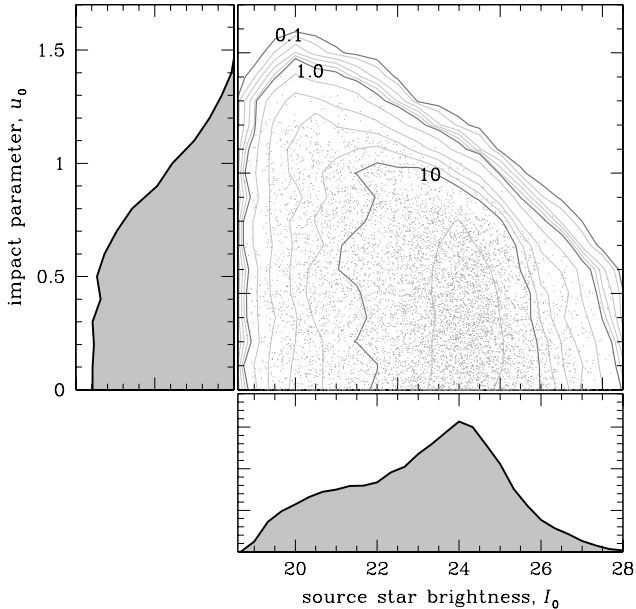


FIG. 1.— Distribution of lensing events in the parameter space of the I -band baseline source brightness, I_0 , and lens-source impact parameter, u_0 . The distribution is for events to be detectable from a lensing survey equipped with a space telescope similar to the *Microblending Space Finder* mission. The contour levels are in relative scale.

event meets the detection criteria. With the new criterion, we find that events can be detected with source brightness down to $I_0 \sim 27$, as shown in the lower panel of Figure 1, where the distribution of I -band baseline source star brightness is presented. With this new range of the source star brightness, the baseline flux of the source star decreases in average while the blended flux remains similar to the previous estimation. As a result, the average value of the blended light fraction, $f_B = F_B / (F_0 + F_B)$, is smaller than the value in Paper I.

4. The last major change is the definition of the resolution angle θ_{res} . In Paper I, we assume that two stars cannot be resolved if the separation between them is less than a fixed value of the diffraction limit (DL) regardless of the flux ratio between the two stars. To describe the experiment more realistically by considering the variation of the resolution angle depending on the relative flux, we set the resolution angle as

$$\theta_{\text{res}} = \begin{cases} 0.5 \text{ FWHM} & \text{if } F_2/F_1 \leq 0.1, \\ [-0.44(F_2/F_1) + 0.54] \text{ FWHM} & \text{otherwise,} \end{cases} \quad (5)$$

where F_1 and F_2 are the fluxes of the brighter and fainter stars, respectively, and $\text{FWHM} \sim 2 \times \text{DL} \sim 0.4''$ corresponds to the diameter of the resolution disk. Then, the resolution angle for two equally bright stars is $\theta_{\text{res}} = 0.1 \text{ FWHM} \sim 0.04''$.⁴ With the adoption of the new definition of the resolution angle, the average blended

⁴ For the *MPF* mission, the pixel size of the detector is $\sim 0.24''/\text{pixel}$, which is bigger than the assumed $\text{DL} = 0.2''$. However, we note that images to be taken by the *MPF* will be dithered and there will be many of them. Therefore, it would be possible to create drizzled images that recover the diffraction limit.

TABLE 1
MPF EVENT RATE

categories	rate
total event rate	3415/yr
– bulge self-lensing events	2192/yr (64.2%)
– disk-bulge events	1223/yr (35.8%)
– stellar lens events	2510/yr (73.5%)
– remnant events	905/yr (26.5%)

NOTE. — Detection rate of microlensing events from the *MPF* survey.

light fraction further decreases compared to that in Paper I.

Based on the simulation, we estimate that the total event rate of the *MPF* survey would be $\Gamma_{\text{tot}} \sim 3500$ events/yr, among which bulge self-lensing and disk-bulge events comprise $\sim 64\%$ and $\sim 36\%$, respectively. The ratio between the events caused by stellar and remnant lenses is $\Gamma_{\star} : \Gamma_{\text{rem}} = 73.5 : 26.5$. We summarize the result of event rate in Table 1.

3. RESULTS

The top panel of Figure 2 shows the distribution of events expected to be detected from the *MPF* survey in the parameter space of the Einstein timescale and blended light fraction. We compare the distribution with those of events expected when the only blending source is the lens (middle panel) and background stars (bottom panel). In each panel, the points marked by bright and dark-tone greyscales represent events caused by stellar and remnant lenses, respectively.

In the case where the dominant source of blending is the lens itself, the distribution has the following distinctive features.

1. First, the region with very little blended light fraction ($f_B \lesssim 0.05$) is densely populated by events caused by remnant lenses, which are dark and thus have no contribution to the blended flux.
2. Second, except for the ones caused by remnants, events are distributed smoothly over the entire range of the blended light fraction.
3. Third, there exists a correlation between the timescale and blending fraction. This correlation arises because heavier lenses tend to be brighter and thus events with longer timescales are more likely to be affected by larger amount of blended flux. We find that the mean timescale is $\langle t_E \rangle \sim 20$ days for stellar-lens events with $f_B \leq 0.1$, while $\langle t_E \rangle \sim 35$ days for events with $f_B \geq 0.9$. However, this correlation is not very strong due to the large dispersions of the Einstein timescale and lens brightness.

In the case where most of the blended flux comes from background stars, on the other hand, the distribution has very different features from those described above. These features are as follows.

1. First, the distribution is not smooth, but divided into two groups of heavily and lightly blended events. The two groups are roughly divided by $f_B \sim 0.5$. This kind of distribution occurs when the number of blended stars

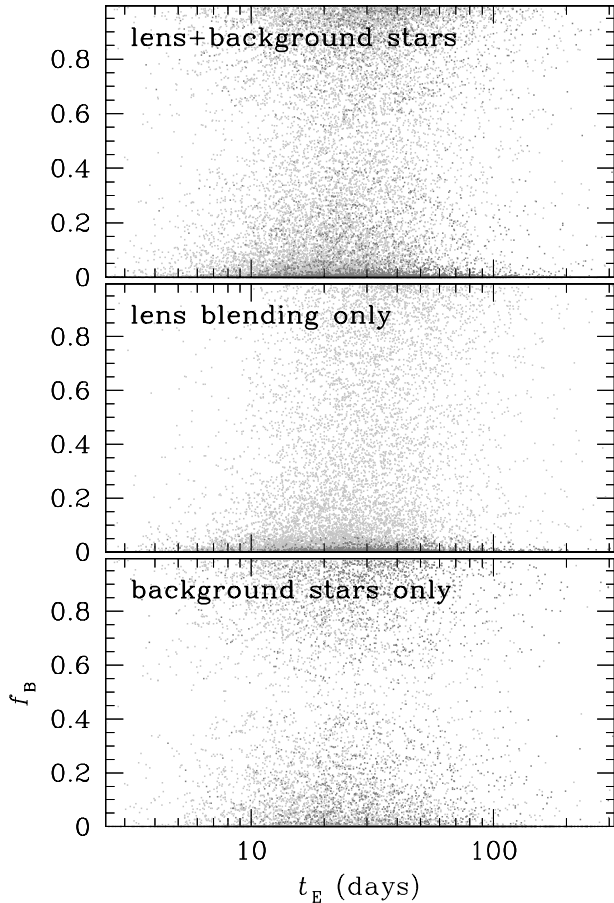


FIG. 2.— Distribution of microlensing events detectable from the *MPF* survey in the parameter space of the Einstein timescale, t_E , and the blended light fraction, f_B (top panel). The other two panels are the distributions expected when the only blending source is the lens (middle panel) and background stars (bottom panel), respectively. In each panel, the points marked by bright and dark-tone greyscales represent the events caused by stellar and remnant lenses, respectively.

in the resolution disk is of an order of one or less. If the number of blended stars is substantially larger (smaller) than this, most events will be distributed in the region of high (low) blended light fraction. We find that the average number of blended stars is ~ 0.42 .

- Another noticeable feature is that both of the events caused by stellar and remnant lenses have similar distributions. This is because there is no contribution of the flux from the lens to the total blended flux.

Considering the characteristics of the distributions for the stellar and lens blending dominated regimes, we find that the distribution of *MPF* events has features of both types of blending. For example, although majority of remnant events are located in the very small f_B region, a considerable fraction of these events are smoothly distributed in a wide range of blended light fraction. In addition, although still events can be divided into two groups of heavily and lightly blended events, the distinction between the two groups is less clear. These characteristics imply that both types of blending are important for events to be detected from the *MPF* survey. This can be seen also in Figure 3, where we plot the distribution of

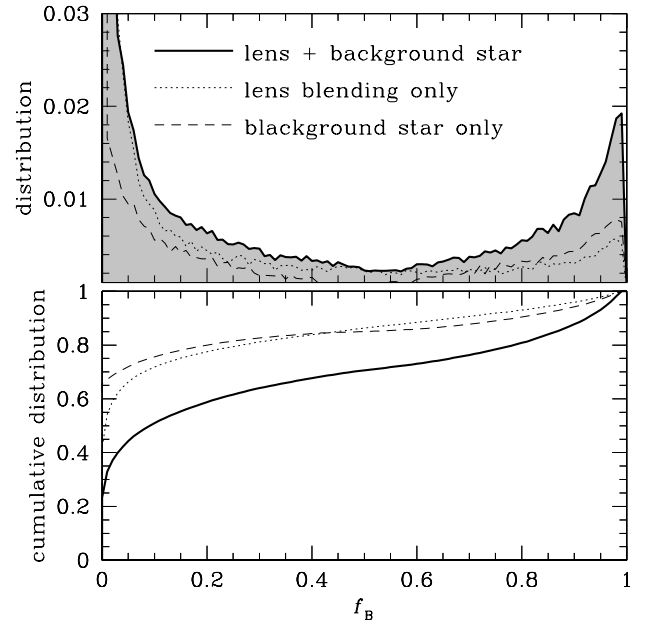


FIG. 3.— Distribution of blended light fractions, f_B , for microlensing events to be detectable from the *MPF* survey (solid curve). The dotted and dashed curves are the distributions when the only blending source is assumed to be the lens and background stars, respectively. Lower panel shows the cumulative distributions.

blended light fraction. From the figure, one finds that both types of blending are nearly equally important.

4. ADDITIONAL ASTROMETRIC INFORMATION

When a source star blended with background stars is gravitationally magnified, the apparent position of the blended image centroid moves toward the source position during the event. The amount of the centroid shift is

$$\Delta r = |\bar{\mathbf{r}} - \bar{\mathbf{r}}_0| = \mathcal{D} |\mathbf{r}_S - \bar{\mathbf{r}}_0|; \quad \mathcal{D} = \frac{(1 - f_B)(A - 1)}{(1 - f_B)(A - 1) + 1}, \quad (6)$$

where \mathbf{r}_S is the position of the source, and $\bar{\mathbf{r}}_0$ and $\bar{\mathbf{r}}$ are the positions of the image centroids before and in the middle of lensing magnification, respectively.

The centroid shift can be measured in other way. Han (2000) and Gould & An (2002) pointed out that the position of the lensed source star, \mathbf{r}_S , instead of the centroid position of the combined image of the source and blend, $\bar{\mathbf{r}}$, can be directly measured on an image obtained by using difference imaging. Difference imaging is an image-subtraction technique to provide accurate photometry and astrometry of variable stars in crowded fields (Tomaney & Crots 1996; Alard & Lupton 1998). In this technique, one first forms a high-quality “template” image. For each of other images (“current” image), one convolves the template image to the same seeing as the current image, translates it so that the two images are geometrically aligned, and linearly rescales its flux so that the two images are photometrically aligned as well. When the convolved template image is subtracted from the current image, all that remain are a set of point spread functions (PSFs) at the locations of stars that experienced light variation. Then, by transforming the coordinates of the source position measured on the subtracted image to the template image, one can measure the positional difference between \mathbf{r}_S and $\bar{\mathbf{r}}_0$. The amount

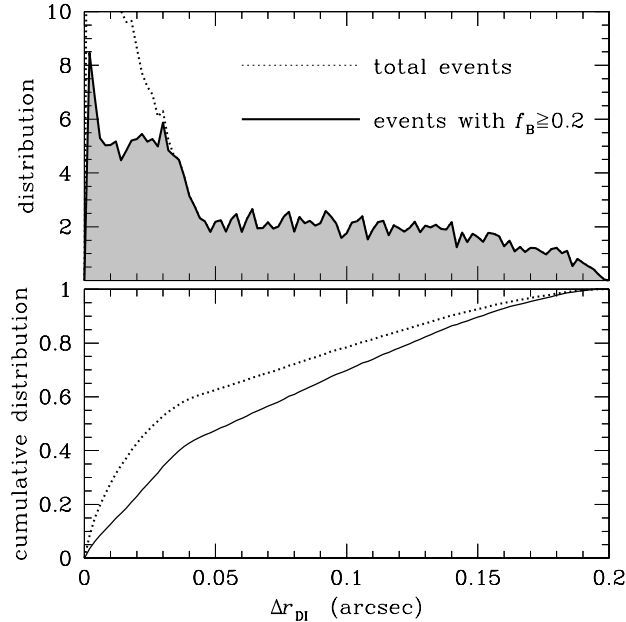


FIG. 4.— Distribution of source star image centroid shifts, Δr_{DI} for microlensing events to be detectable from the *MPF* survey. The dotted and solid curves are for all events and those with blended light fraction $f_{\text{B}} \geq 0.2$, respectively. Lower panel shows the cumulative distributions.

of the centroid shift measured in this way is related to the shift measured directly on two regular images by

$$\Delta r_{\text{DI}} = |\mathbf{r}_{\text{S}} - \bar{\mathbf{r}}_0|. \quad (7)$$

We note that the centroid shift measured in this way is always larger than the shift in equation (6) because $\mathcal{D} < 1.0$.

Astrometric information of the centroid shift might be important in distinguishing events blended by the lens and background stars. This is because typical separation between the source and blended background star, which is of an order of 10^{-2} arcsec, is much larger than the separation between the source and lens, which is of an order of 10^{-4} arcsec. Then, if no centroid shift is detected within the astrometric precision of the centroid shift measurement despite that blending is noticed from the lightcurve, the chance that the lens is the blending source is very high. Figure 4 shows the distribution of the centroid shifts for events detectable by the *MPF* survey.

We investigate the usefulness of the astrometric information in sorting out events where most of the blended flux is attributable to the lens. For this, we calculate the fraction of blended flux from background stars, F_* , out of the total blended flux for events where blending is noticed with $f_{\text{B}} \geq 0.2$ but no centroid shift is detected within the astrometric uncertainty. The astrometric uncertainty of the centroid shift measurement is

$$\sigma_{\text{ast}} \sim \frac{\text{FWHM}}{N_{\nu}^{1/2}}, \quad (8)$$

where N_{ν} is the photon count. We assume that the centroid shift is measured from difference imaging, i.e. $\Delta r_{\text{I}} = |\mathbf{r}_{\text{S}} - \bar{\mathbf{r}}_0|$. Despite the absence of atmosphere, difference imaging on space-based observation may not be simple due to variations in the PSF profile from image to image caused by temporal variations in the thermal load on spacecraft (Gilliland et al 2000). Furthermore, the *MPF* mission may suffer from un-

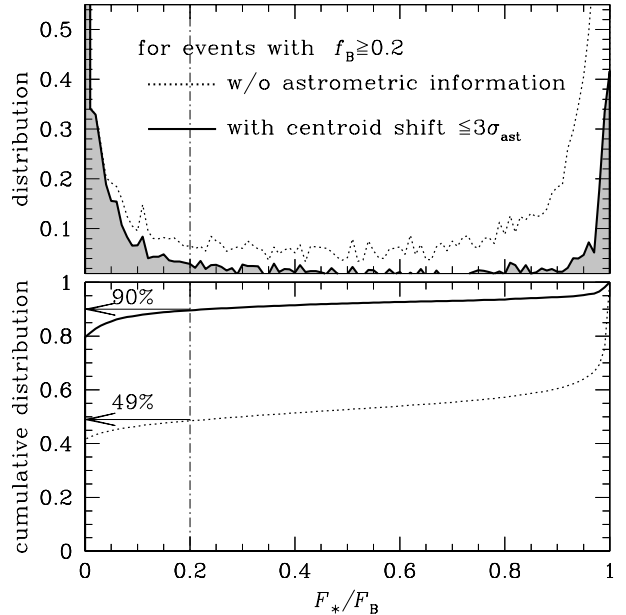


FIG. 5.— Distribution of the fractions of the blended flux from background star, F_* , out of the total blended flux, F_{B} , for *MPF* microlensing events with the blended light fraction $f_{\text{B}} \geq 0.2$ (dotted curve). Solid curve is the distribution for events that are additionally filtered out with astrometric information under the condition that the measured source star image centroid shift, Δr_{DI} , is less than 3 times of the astrometric uncertainty, σ_{ast} . Lower panel shows the cumulative distributions.

dersampling of the PSF which further complicates the geometric alignment procedure which involve interpolation of undersampled PSFs. To account for these possible additional sources of uncertainty in astrometric measurement, we consider only centroid shifts with $\Delta r_{\text{DI}} > 3\sigma_{\text{ast}}$ can be firmly detected.

In Figure 5, we present the resulting distributions of the fraction F_*/F_{B} . Dotted curve is for events with blended light fractions $f_{\text{B}} \geq 0.2$ and solid curve is the distribution for events that are additionally filtered out with astrometric information under the condition that the measured centroid shift is $\Delta r_{\text{DI}} \leq 3\sigma_{\text{ast}}$. We note that the blended flux from background stars works as a contaminant to the flux from the lens, and thus small ratio of F_*/F_{B} implies that the blended flux is mostly from the lens. From the distributions, we find that blended flux of nearly half (49%) of all events with $f_{\text{B}} \geq 0.2$ is contaminated by the flux from background stars by more than $F_*/F_{\text{B}} = 20\%$. However, for the sample of events filtered out by using the additional astrometric information, it is found that only a minor fraction ($\sim 10\%$) of events are contaminated by background stellar blending. We also find that this sample of events comprises $\sim 22\%$ of all *MPF* lensing events. Considering the total event rate of ~ 3500 events/yr of the survey, the rate of these events is ≥ 700 events/year, which is large enough for the statistical analysis of the lens populations.

5. CONCLUSION

We investigated the effect of blending in future gravitational microlensing surveys using a 1 m class space telescope. For this, we carried out simulation of Galactic bulge microlensing events to be detected from the proposed *MPF* lensing survey by imposing realistic observational conditions and detection criteria. From this simulation, we found that the contribu-

tion of the flux from blended background stars to the total blended flux is equivalent to that of the lens itself, implying that characterizing lenses from the analysis of the blended flux would not be easy. However, with the additional astrometric information of the source star image centroid shift, we found that it would be possible to isolate events for which most of the blended flux is attributable to the lens. For the sample of events obtained by imposing a criterion that the centroid shift should be less than three times of the astrometric uncertainty among the events for which blending was noticed with

blended light fractions $f_B > 0.2$, we estimated that the contamination of the blended flux by background stars would be less than 20% for most ($\sim 90\%$) of the sample events. The expected rate of these events is $\gtrsim 700$ events/yr, which is large enough for the statistical analysis of the lens populations.

This work was supported by the grant (C00072) of the Korea Research Foundation.

REFERENCES

- Abe, F., et al. 2003, *A&A*, 411, L493
 Alard, C., & Lupton, R. H. 1998, *ApJ*, 503, 325
 Albrow, M. D., et al. 1999, *ApJ*, 522, 1011
 Alcock, C., et al. 1993, *Nature*, 365, 621
 Aubourg, E., et al. 1993, *Nature*, 365, 623
 Beaulieu, J.-P., et al. 2006, *Nature*, 439, 437
 Bennett, D. P. 2004, *BAAS*, 205, 11.26
 Bennett, D. P., & Rhie, S. H. 2002, *ApJ*, 574, 985
 Bond, I. A., et al. 2001, *MNRAS*, 327, 868
 Bond, I. A., et al. 2004, *ApJ*, 606, L155
 Di Stefano, R., & Esin, A. A. 1995, *ApJ*, L1
 Evans, N. W. 1994, *ApJ*, 437, L31
 Field, D. L., et al. 2003, *ApJ*, 596, 1305
 Gilliland, R. L., et al. 2000, *ApJ*, 545, L47
 Goldberg, D. M. 1998, *ApJ*, 498, 156
 Gould, A. 2000, 535, 928
 Gould, A. 2001, *PASP*, 113, 903
 Gould, A., et al. 2006, *ApJ*, 644, L37
 Gould, A., & An, J. H. 2002, 565, 1381
 Gould, A., Bahcall, J. N., & Flynn, C. 1997, 482, 913
 Gould, A., & Loeb, A. 1992, *ApJ*, 396, 104
 Han, C. 2000, *Journal of Korean Astro. Soc.*, 33, 89
 Han, C. 2005, *ApJ*, 633, 414
 Han, C., & Gould, A. 1995a, *ApJ*, 447, 53
 Han, C., & Gould, A. 1995b, *ApJ*, 449, 521
 Han, C., & Gould, A. 2003, *ApJ*, 592, 172
 Holtzman, J. A., Watson, A. M., Baum, W. A., Grillmair, C. J., Groth, E. J., Light, R. M., Lynds, R., & O'Neil, E. J. 1998, *AJ*, 115, 1946
 Kiraga, M., & Paczyński, B. 1994, *ApJ*, 430, L101
 Mao, S., & Paczyński, B. 1991, *ApJ*, 374, L37
 Paczyński, B. 1986, *ApJ*, 304, 1
 Tomaney, A. B., & Crotts, A. P. S. 1996, *AJ*, 112, 2872
 Udalski, A., Szymański, M., Kałużny, J., Kubiak, M., Krzemiński, W., Mateo, M., Preston, G. W., & Paczyński, B. 1993, *Acta Astron.*, 43, 289
 Udalski, A., et al. 2005, *ApJ*, 628, L109
 Witt, H. J. 1995, *ApJ*, 449, 42
 Woźniak, P. R., & Paczyński, B. 1997, *ApJ*, 487, 55
 Zhao, H., Spergel, D. N., & Rich, R. M. 1995, *ApJ*, 440, L13